Ferroan Anorthosite 60025 – A Lunar Breccia. Torcivia M.A.[1] and Neal C.R.[1] [1]Dept. Civil & Env. Eng. & Earth Sciences, University of Notre Dame, Notre Dame IN, 46556; mtorcivi@nd.edu

Introduction: Ferroan anorthosites (FANs) are hypothesized to have formed from the cohesion of plagioclase flotation cumulates that crystallized from the Lunar Magma Ocean (LMO) early in the Moon's formation [1]. As products of the LMO, FANs are believed to represent the primordial lunar crust [2] and are the only samples we have that are direct LMO products. The timing of FAN formation is therefore directly tied to constraining the age of the Moon and its early differentiation. Lunar sample 60025 is a member of the FANs, and previous geochronologic studies have used their ages to estimate the age of the Moon and the earliest lunar crust [3]. Sample 60025 is also unique in that it has two distinct Sm-Nd crystallization ages: 4.44±0.02 Ga [3] and 4.367±0.011 Ga [4]. The younger age [4] introduces the problem of extending LMO activity beyond what most models of the LMO consider feasible and brings into question our understanding of FAN petrogenesis. While possible to reconcile the issues raised by a young age by rethinking FAN formation (e.g. serial magmatism) or LMO systematics (e.g. quenched lid and tidal heating extending LMO crystallization time), an alternative explanation can be found in the detailed petrology preserved in the thin sections of 60025.

Methods: Five thin sections of 60025 are available for study at Notre Dame: 60025,21; ,134; ,269; ,273; and ,274. Photomicrographs of each thin section in cross polar (XPL), plane polar (PPL), and reflected (REF) light were created using a Nikon camera connected to a Nikon petrographic microscope and then stitching the individual images together using Microsoft Image Composite Editior. These photomicrographs serve as both a navigation map for subsequent analyses and provide context for those in-situ analyses. Major and minor element data was collected via electron microprobe (EMP) analysis using a Cameca SX-50 electron microprobe at the University of Notre Dame. Plagioclase analyses were recorded in core-rim pairs while mafic analyses were one per crystal due to their small sizes. Trace element data was collected via laser ablation (LA) ICP-MS analysis using an Element 2 ICP-MS instrument connected to a New Wave Research UP-213 laser delivery system (also at the University of Notre Dame). Laser spot size ranged from 40-100 microns. The CaO data collected by electron microprobe was used as the internal standard for both plagioclase and pyroxene analyses, as was the external galss standard NIST-612. Raw data were reduced using the GLITTER software [5].

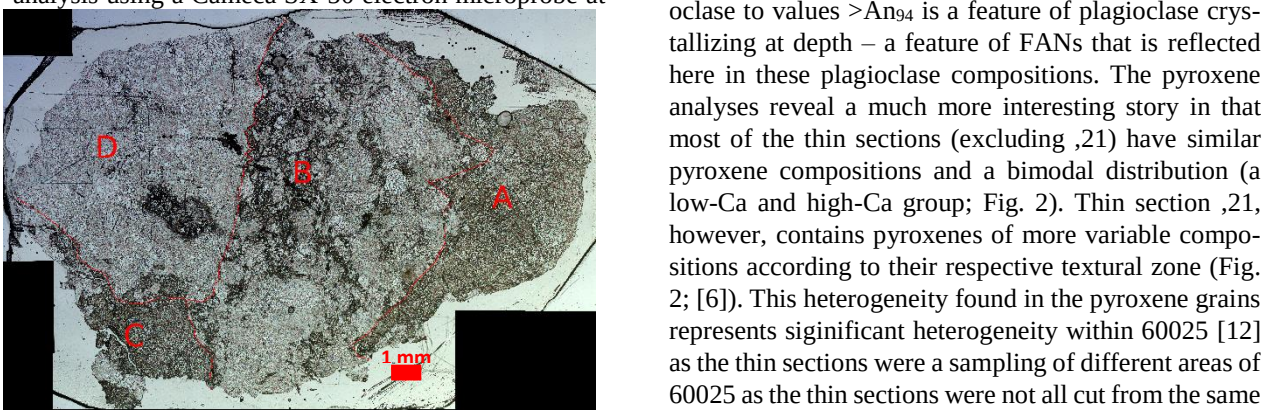

Figure 1: PPL image of 60025,21.

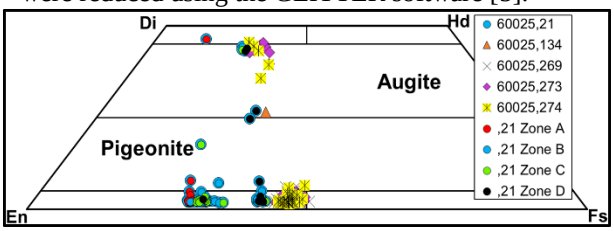

Figure 2: EMP analysis of pyroxene grains from all thin setions.

Results and Discussion: Initial petrographic observations of the thin sections reveal that 60025 is severely brecciated (Fig. 1). All thin sections (excluding ,21) show a majority (>90%) plagioclase with minor pyroxene and other assorted mafics (sans olivine). Section 60025,21 differs from the others in its higher amount of mafic material, presence of olivine, and 4 distinct textural zones (Fig. 1) identified by [6]. The initial petrography indicates the petrogenesis of 60025 was not as simple as its 'pristine' label [7,8] would imply.

Electron Microprobe. EMP analyses of the plagioclase grains show that the plagioclase in 60025 is very anorthositic (>An_{95}) with the cores of the grains showing a slight negative correlation with FeO weight percent and the rims showing a random "shotgun spread". It has been suggested by [9] that the restriction of plagioclase to values >An_{94} is a feature of plagioclase crystallizing at depth – a feature of FANs that is reflected here in these plagioclase compositions. The pyroxene analyses reveal a much more interesting story in that most of the thin sections (excluding ,21) have similar pyroxene compositions and a bimodal distribution (a low-Ca and high-Ca group; Fig. 2). Thin section ,21, however, contains pyroxenes of more variable compositions according to their respective textural zone (Fig. 2; [6]). This heterogeneity found in the pyroxene grains represents siginificant heterogeneity within 60025 [12] as the thin sections were a sampling of different areas of 60025 as the thin sections were not all cut from the same parent (see the family tree in [10]).

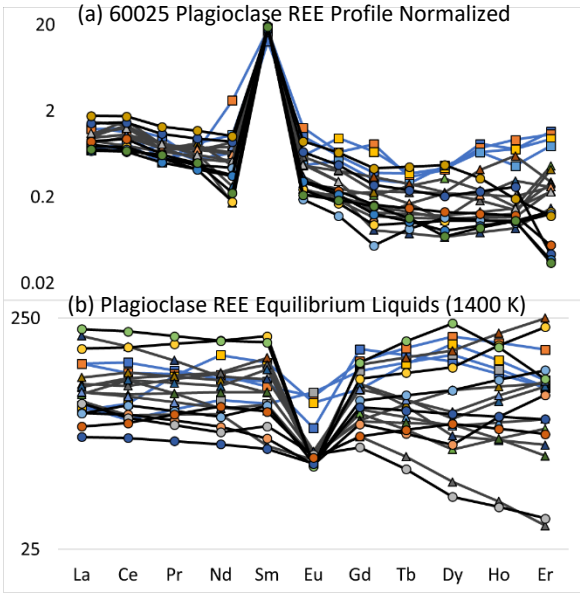

Figure 3: REE profiles of plagioclase (a) and their respective equilibrium liquids (b). Black lines and circles refer to 60025,273; Grey lines and triangles refer to 60025,269; and Blue lines and squares refer to 60025,21.

LA-ICP-MS. Laser ablation of plagioclase and pyroxene grains were conducted on three thin sections of 60025: ,273; ,269; and ,21. Rare earth element (REE) profiles of plagioclases show a general agreement between thin sections analyzed being light REE enriched with a characteristic positive Eu anomaly (Fig. 3a). The calculated equilibrium liquids for each grain (using the method from [11]) show that not all plagioclase grains are consistent with crystallizing from the LMO based on their modelled REE profiles [13] (Fig. 3b). Section ,21 for instance has plagioclase grains enriched in HREE relative to their LREE, which is inconsistent with crystallizing out of an LMO liquid [13]. Figure 4 graphs La vs Er equilibrium liquid concentration for multiple FANs [14] including 60025 from this study. Here parts of 60025 plot near the very end of LMO crystallization while other points plot well above expected LMO values further supporting the presence of non-LMO components within the 60025 breccia. The pyroxene analyses also show strong evidence for heterogeneity between grains. Particularly interesting are two pyroxene grains which show a positive Eu anomaly in both their grain analyses and calculated equilibrium liquids (profiles found in [15]). These grains have REE profiles that plot sub-parallel to the other orthopyroxene grains with the exception of their unusual positive Eu peak. The presecnce of such a Eu anomaly in a lunar pyroxene is unprecedented and inconsistent with crystallization from the LMO [15]. The equilibrium liquids of the other pyroxene grains analyzed show multiple different profile types including LREE enriched profiles, flat REE profiles (i.e. neither LREE enriched nor depleted), and LREE depleted profiles. These differences in their equilibrium liquids reflect a distinction between their respective parent liquids.

Conclusions: Lunar sample 60025 is a breccia consisting of both LMO and non-LMO derived material. It is composed of multiple different FAN lithologies. The discordant ages recorded by [3] and [4] coupled with the brecciated texture of the thin sections, different textural zones in thin section ,21, distinct major element composition groupings of the pyroxenes, and multiple different equilibrium liquid REE profiles of plagioclase and pyroxene grains support the hypothesis that 60025 represents a 'mixture of several FAN lithologies' as hypothesized by [12]. Therefore, the discordant ages which previously called into question LMO systematics could be reconciled as merely a representation of sampling of different materials – neither age is incorrect, but neither may represent a true FAN crystallization age due to mixing of different lithologies.

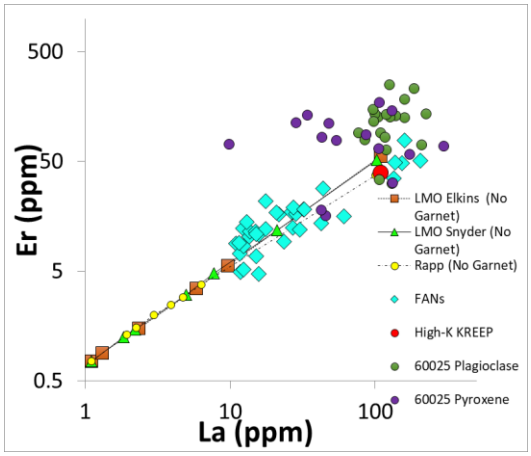

Figure 4: La vs Er plot of equilibrium liquids along an expected trend line. Based on data from [15]

References: [1] Toksöz M. & Solomon S. (1973) EMP 7, 251-278. [2] Dowty E. et al. (1974) EPSL 24, 15-25. [3] Carlson R. & Lugmair G. (1988) EPSL 90, 119-130. [4] Borg L. et al. (2011) *Nature* 477, 70-72. [5] van Achterbergh E. et al. (2001) *Mineralogical Association of Canada, Short Course* 29, 239–243. [6] Ryder G. (1982) GCA 46, 1591-1601. [7] Warren P. & Wasson J. (1977) PLSC 8, 2215-2235. [8] Warren P. (1993) *American Mineralogist* 78, 360-376. [9] Nekvasil H. et al. (2015) GRL 10, 573-579. [10] Meyer C. (2011) *Lunar Sample Compendium* 60025. [11] Hui H. et al. (2011) GCA 75, 6439-6460. [12] James O. et al. (1991) PLPSC 21, 63-87. [13] Neal C. & Davenport J. (2014) LPSC 45, #1181. [14] Neal C. & Draper D. (2016) LPSC 47, #1165. [15] Torcivia M. & Neal C. (2017) LPSC 48, #1471.